Atmos. Chem. Phys. Discuss., 14, 19431–19468, 2014
www.atmos-chem-phys-discuss.net/14/19431/2014/
doi:10.5194/acpd-14-19431-2014

Atmospheric Chemistry and Physics Discussions

OH initiated heterogeneous oxidation of tris-2-butoxyethyl phosphate: implications for its fate in the atmosphere

Y. Liu, L. Huang, S.-M. Li, T. Harner, and J. Liggio

Atmospheric Science and Technology Directorate, Science and Technology Branch, Environment Canada, Toronto, M3H 5T4, Canada

Received: 10 July 2014 – Accepted: 14 July 2014 – Published: 29 July 2014

Correspondence to: J. Liggio (john.liggio@ec.gc.ca)

Published by Copernicus Publications on behalf of the European Geosciences Union.

Abstract

A particle-phase relative rates technique is used to investigate the heterogeneous reaction between OH radicals and tris-2-butoxyethyl phosphate (TBEP) at 298 K by combining Aerosol Time-of-Flight Mass Spectrometry (C-ToF-MS) data and Positive Matrix Factor (PMF) analysis. The derived second-order rate constants (k_2) for the heterogeneous loss of TBEP is (4.44 ± 0.45) × 10^{-12} cm^3 $molecule^{-1}$ s^{-1}, from which an approximate particle-phase lifetime was estimated to be 2.6 (2.2–2.9) days. However, large differences in the relative rate constants for TBEP to a reference compound were observed when comparing internally and externally mixed TBEP/organic particles, and upon changes in the RH. The heterogeneous degradation of TBEP was found to be depressed or enhanced depending upon the particle mixing state and phase, highlighting the complexity of heterogeneous oxidation in the atmosphere. The effect of gas-particle partitioning on the estimated overall lifetime (gas + particle) for several organophosphate esters (OPEs) was also examined through the explicit modeling of this process. The overall atmospheric lifetimes of TBEP, tris-2-ethylhexyl phosphate (TEHP) and tris-1,3-dichloro-2-propyl phosphate (TDCPP) were estimated to be 1.9, 1.9 and 2.4 days respectively, and are highly dependent upon particle size. These results demonstrate that modeling the atmospheric fate of particle phase toxic compounds for the purpose of risk assessment must include the gas-particle partitioning process, and in future include the effect of other PM components on the evaporation kinetics and/or the heterogeneous loss rates.

1 Introduction

The effects of fine particles on the atmosphere, climate, and public health are among the central topics in current environmental research (Pöschl, 2005). These effects are closely related to the particle size, morphology, and composition (Pöschl, 2005; Kolb and Worsnop, 2012). In this regard, heterogeneous reactions can modify not only

particulate composition, but also the physical properties of particles including size, density and morphology, thereby affecting their optical and hygroscopic properties (Ravishankara, 1997; George and Abbatt, 2010a). Consequently, heterogeneous reaction kinetics are key parameters in both atmospheric chemistry and climate modeling; they are used to adequately compute the trace gas and particulate matter content of the atmosphere (Kolb et al., 2010), to evaluate the importance of heterogeneous reactions in the atmosphere (Zhang and Carmichael, 1999), and in the assessment of organic aerosol lifetime (Zhou et al., 2012).

Significant progress has been made with respect to the laboratory measurement of trace gas uptake to the surface of organic and inorganic particles (Mogili et al., 2006; Qiu et al., 2011; Y. Liu et al., 2012; Liggio et al., 2011; Romanias et al., 2012; Tang et al., 2010; Ndour et al., 2008; Hanisch and Crowley, 2003; Frinak et al., 2004; Ullerstam et al., 2003; Han et al., 2013; Badger et al., 2006; Zhou et al., 2012; Abbatt et al., 2012; Kolb et al., 2010; Crowley et al., 2010). In comparison to the uptake of stable trace gases, heterogeneous uptake coefficients for short-lived radicals including OH, Cl, and NO_3 (Hearn and Smith, 2006; George et al., 2007; Lambe et al., 2007; McNeill et al., 2007, 2008; Smith et al., 2009; Kessler et al., 2010, 2012; Renbaum and Smith, 2011; Kessler et al., 2012; C. Liu et al., 2012; Sareen et al., 2013) are limited at the present time. Given that organic aerosols (OA) comprise 10–90 % of the aerosol mass in the lower troposphere (Zhang et al., 2011; Kanakidou et al., 2005), heterogeneous reactions of radicals with OA can have important implications for organic aerosol properties. It has been demonstrated that the reactive uptake of OH leads to increases in density, CCN activation (George and Abbatt, 2010b) and optical extinction (Cappa et al., 2011) of OA, and has been postulated as a potential route to increased organic oxygen content (ie: increased O/C ratio) (George and Abbatt, 2010a; Heald et al., 2010). Thus, there is a growing interest in understanding the mechanisms and kinetics associated with the chemical transformation of OA in the lower troposphere through reactions with these radicals (Hearn and Smith, 2006).

Donahue et al. (2005) and Hearn and Smith (2006) have developed a mixed-phase relative rates technique for measuring particle reaction kinetics. In this method, the rate constant for the second order heterogeneous loss of a compound of interest (ie: k_2) is determined from the decrease in its particle-phase concentration as a function of oxidant exposure. Oxidant exposure is in turn derived by the measured loss of a gas-phase reference compound, applying known second-order gas-phase rate constants (k_2) toward the oxidant. Using this method, many studies have reported the uptake coefficients of O_3, OH, Cl, and NO_3 on various organic aerosols (Hearn and Smith, 2006; George et al., 2007; Lambe et al., 2007; McNeill et al., 2007, 2008; Smith et al., 2009; Kessler et al., 2010, 2012; Renbaum and Smith, 2011; C. Liu et al., 2012; Sareen et al., 2013). In most of these studies, the concentration of the particle-phase compound of interest was measured with an Aerosol Mass Spectrometer (AMS), utilizing specific mass spectral fragments as a tracer for the particulate compound, while the gaseous reference compound was usually monitored with other instrumentation. In our previous work, we demonstrated that the larger the tracer fragment chosen, the larger the k_2 value that is derived if the products are highly similar to the reactant and a unit mass resolution (UMR) AMS is utilized (Liu et al., 2014b). It was also demonstrated that an approach using PMF analysis improves the accuracy of the rate constant determination for selected organophosphate flame retardants found in particles (Liu et al., 2014a).

Organophosphate esters (OPEs) have been used extensively worldwide as flame retardants, plasticizers, antifoaming agents, and additives (Regnery and Püttmann, 2009). The global consumption of OPEs is expected to increase since they have been identified as possible substitutes for some bromine-containing flame retardants (BFRs) (Reemtsma et al., 2008; Dodson et al., 2012). Recent field measurements suggest that OPEs are persistent in air and can undergo medium to long range transport (Möller et al., 2012). Given that many OPEs are considered toxic (EPA, 2005; WHO, 2000; Dishaw et al., 2011) it is necessary to assess their environmental behavior and fate, in order to understand the risks associated with these compounds. However, the

degradation kinetics for particle bound OPEs is not available, but will be important for assessing the persistence of those OPEs which are primarily in the particle phase.

As a flame retardant, tris-2-butoxyethyl phosphate (TBEP) is used mainly as self leveling agent in floor polishes, solvent in some resins, viscosity modifier in plastics, antifoam and plasticizer in synthetic rubber, plastics and lacquers (IPCS, 2000; Verbruggen et al., 2005). The world production has been estimated to be 5000–6000 tons (Verbruggen et al., 2005). TBEP appears to be rapidly biodegradable in soil, sediments and surface waters (IPCS, 2000). Based upon the rate constant estimated via the structure activity relationship (SAR) method, its atmospheric lifetime in the gas-phase should be less than 2.5 h. However, TBEP has been measured in both house dust (Dodson et al., 2012; Ali et al., 2012; Cequier et al., 2014) and ambient particles (Möller et al., 2012; Salamova et al., 2013). It has also been detected in remote regions, although its concentration is lower than other OPEs (Möller et al., 2011, 2012; Salamova et al., 2014). This suggests that TBEP may undergo particle-bound long or medium-range transport and that the lifetime of particle-bound TBEP should be longer than that expected in the gas phase. Currently, particle-phase degradation kinetics for TBEP is unavailable.

In the current study a particle-phase relative rates technique (Donahue et al., 2005) (as opposed to mixed-phase) for the heterogeneous oxidation is used to derive the heterogeneous rate constant for TBEP towards OH radical. In addition, the influence of particle mixing state on the heterogeneous oxidation of TBEP is investigated for the TBEP-Citric acid system. Finally, the derived kinetic parameters are used as inputs into a partitioning model as a means to estimate the overall atmospheric lifetime of OPEs including TBEP, tris-2-ethylhexyl phosphate (TEHP), triphenyl phosphate (TPhP) and tris-1,3-dichloro-2-propyl phosphate (TDCPP).

2 Experimental details

2.1 Flow tube experiments

A detailed schematic representation of the experimental system and the flow tube reactor utilized in this study have been described elsewhere (Liu et al., 2014a, b), and is shown in Fig. S1 in the Supplement. Internally mixed TBEP and CA (TBEP-CA), TBEP and ammonium nitrate (TBEP-AN), CA and AN (CA-AN), and TBEP, CA and AN (TBEP-CA-AN) particles were generated via atomization (model 3706, TSI), dried through a diffusion drier and size-selected with a differential mobility analyzer (DMA) (model 3081, TSI) with a final mode surface-weighted mobility diameter (D_m) of approximately 210 nm. Pure CA particles of the same size were generated simultaneously with a separate atomizer, diffusion drier and DMA for externally mixed particle experiments. Although NH_4NO_3 may have an influence on the reactivity of TBEP when compared to pure TBEP, there are two reasons for measuring the rate constants of TBEP using internally mixed TBEP-AN. Firstly, the generation of a particle stream with a high and stable particle concentration is facilitated when using a non-volatile inorganic seed internally mixed TBEP-AN. Secondly, internally mixed particles (with an inert inorganic salt) is more representative of conditions in the atmosphere, where TBEP will be internally mixed with a range of other species.

OH radicals were produced by the photolysis of O_3 at 254 nm in the presence of water vapor. O_3 was generated by passing zero air through an O_3 generator (OG-1, PCI Ozone Corp.). The O_3 concentration in the reactor was measured using an O_3 monitor (model 205, 2B Technologies) and ranged from 0–1000 ppbv. Relative humidity (RH) in the reactor was (30 ± 3) % and maintained by varying the ratio of wet to dry air used as an air source. The temperature was maintained at 298 K.

In our previous work, we measured the heterogeneous rate constants ($k_{2,OH}$) for several OPEs, (TPhP, TEHP and TDCPP,) with the mixed-phase relative rates technique, which utilized methanol as a reference compound for the OH concentration determination (Liu et al., 2014b). Unfortunately, the oxidized products of TBEP significantly

contribute to the methanol signal when measured with a proton-transfer mass spectrometer (PTR-MS). Therefore, particle-phase citric acid (CA), whose reaction kinetics were investigated previously (Liu et al., 2014a), was utilized as an OH radical reference compound in this study. A PMF analysis was performed to differentiate the signals of TBEP, CA, and the corresponding oxidation products. The steady-state OH exposures were varied from 0 to $\sim 8.0 \times 10^{11}$ molecules cm^{-3} s^{-1} which was estimated on the basis of the decay of CA from its reaction with OH and the diffusion-corrected k_2 of $(3.31 \pm 0.29) \times 10^{-12}$ cm^3 $molecule^{-1}$ s^{-1} for CA at 298 K and (30 ± 3) % RH (Liu et al., 2014a).

Table 1 summarizes the types of particles introduced into the reactor and the associated objectives of each experiment. Specifically, in Experiment I, the oxidation of internally mixed CA-AN and internally mixed TBEP-AN was carried out individually by alternating particle sources and oxidation conditions thus providing a means to directly obtain reference spectra (concentration profiles) for PMF analysis and to assess the suitability of the PMF technique to separate the signals of CA and TBEP. In Experiment II, pure CA and internally mixed TBEP-AN (ie: CA externally mixed with TBEP-AN) were oxidized simultaneously to derive the kinetics of TBEP. In Experiment III, internally mixed CA-TBEP or CA-TBEP-AN was oxidized to investigate the influence of mixing state on the reaction kinetics. An experiment at elevated RH (57 ± 2) % was also performed using internally mixed CA-TBEP-AN to investigate the influence of RH on the mixing state and subsequently the reactivity.

Control experiments demonstrated that O_3 exposure did not lead to the decomposition of TBEP or CA. To exclude the possibility of TBEP photolysis by the 254 nm light, the particles were illuminated to measure the initial concentration of CA and TBEP prior to OH introduction. TBEP (94 %, TCI America Inc.), analytic grade CA (EM, Germany) and NH_4NO_3 (Sigma-Aldrich) were used as received. 18.2 MΩ water was used as a solvent.

2.2 PMF analysis and kinetic calculations

.

The C-ToF-AMS data of OA were analyzed with the PMF Evaluation Toolkit (PET) v2.05 (Paatero, 1997; Paatero and Tapper, 1994) to separate the signals of TBEP, CA, and their corresponding oxidation products. The parameters used as input for the PMF analysis have been described previously (Liu et al., 2014a). The factor profiles (mass spectra) were compared with the NIST mass spectra of pure TBEP and CA, as well with those measured through direct atomization into the C-ToF-AMS. The extracted signals of TBEP and CA were used for kinetics calculations.

The relative rates technique is widely used for gas-phase and mixed-phase (ie: heterogeneous) reaction kinetics studies with several advantages: (1) no absolute concentration measurements are required, (2) impurities do not generally interfere with the measurements, (3) the experiments can be carried out in the presence of several reaction partners, and (4) the initiation of radical chains during the reaction process does not affect the measurements (Barnes and Rudzinski, 2006). Similar to gas-phase or mixed-phase relative rates technique, TBEP and CA are externally mixed (to avoid the possible influence of mixing state on the reactivity of CA) and simultaneously exposed to OH radicals. Thus, the rate of change in the concentration of reactants for a second-order reaction is given by,

$$-\frac{\mathrm{d}c_{\mathrm{TBEP}}}{\mathrm{d}t} = k_{2,\mathrm{TBEP}} c_{\mathrm{TBEP}} c_{\mathrm{OH}} \quad (1)$$

$$-\frac{\mathrm{d}c_{\mathrm{CA}}}{\mathrm{d}t} = k_{2,\mathrm{CA}} c_{\mathrm{CA}} c_{\mathrm{OH}} \quad (2)$$

from which Eq. (3) is obtained by the ratio of Eqs. (1)/(2).

$$\frac{\mathrm{d}c_{\mathrm{TBEP}}}{c_{\mathrm{TBEP}}} = \frac{k_{2,\mathrm{TBEP}}}{k_{2,\mathrm{CA}}} \frac{\mathrm{d}c_{\mathrm{CA}}}{c_{\mathrm{CA}}} \quad (3)$$

And thus,

$$\log \frac{c_{\mathrm{TBEP}}}{c_{\mathrm{TBEP},0}} = \frac{k_{2,\mathrm{TBEP}}}{k_{2,\mathrm{CA}}} \log \frac{c_{\mathrm{CA}}}{c_{\mathrm{CA},0}} = k_{\mathrm{r}} \log \frac{c_{\mathrm{CA}}}{c_{\mathrm{CA},0}} \quad (4)$$

where c_i and $k_{2,i}$ are the concentration (molecules cm^{-3}), and the second-order rate constant of the compound i (CA or TBEP) (cm^3 molecule^{-1} s^{-1}), respectively. The term k_{r} is the relative rate constant defined as the ratio of second-order rate constants for TBEP and CA towards OH radical oxidation, and is obtained from the slope of the plot of $\log c_{\mathrm{TBEP}}/c_{\mathrm{BEP},0}$ vs. $\log c_{\mathrm{CA}}/c_{\mathrm{CA},0}$.

3 Results and discussion

3.1 Reference spectra for PMF analysis (Exp. I)

Reference spectra are used to properly interpret the PMF results and to confirm that the signals are correctly separated for internally or externally mixed particles. Individual oxidation experiments were performed separately for TBEP-AN and CA-AN by alternating particle sources and oxidation conditions. PMF analysis was then performed using the combined AMS data of both TBEP-AN and CA-AN to provide reference spectra and to assess the ability of PMF to correctly separate the signals of TBEP and CA from their corresponding products. To ensure the same OH exposure, the particle sources of TBEP and CA were alternately introduced into the reactor with the same flow rate, RH and O_3 concentration.

In our previous study, a two-factor solution adequately explained the unreacted CA and products for CA oxidation (Liu et al., 2014a), suggesting that a two-factor solution for TBEP oxidation is also likely. Consequently 4 factors were chosen in the PMF analysis here. Figures 1 and 2 show the 4-factor solution for the oxidation of internally mixed TBEP-AN and internally mixed CA-AN when individually exposed to different OH

concentrations (ie: Exp. I). The Q/Q_{exp} variance is 99.6 % for a 4-factor solution, resulting in a small residual. In Fig. 1, the number "0" represents an OH exposure equal to zero, while the numbers from "1" to "6" represent a step-wise OH exposure decrease from $(7.8 \pm 0.8) \times 10^{11}$ to $(8.5 \pm 0.8) \times 10^{10}$ molecules cm^{-3} s^{-1}. The shift from red to blue color represents the change of particle source (from internally mixed CA-AN to internally mixed TBEP-AN). The error bars indicate the uncertainty in the rotations of the PMF analysis.

As demonstrated in Fig. 1, factor 1 (attributed to the CA reactant) accounts for (95.6 ± 2.4) % of the OA mass, and factor 3 (attributed to TBEP) accounts for (95.9 ± 2.7) % of the OA mass in the absence of OH radical. However, a small amount (3.2 ± 1.9) % of Factor 2, which may originate from organic impurities in water and/or NH_4NO_3, is always present in the CA-AN and TBEP-AN experiments prior to the OH exposure. It may also possibly be the result of an inability of PMF to properly separate factors due to the model uncertainty. When the particles are exposed to OH radicals, consumption of both CA and TBEP is significant and positively correlated with the OH exposure. Concurrently, the signals of CA (factor 1) and TBEP (factor 3) are anti-correlated with factor 2 and factor 4, respectively. As demonstrated in Fig. 1, oxidation of TBEP also results in a minor contribution (~ 10 % at the highest OH exposure) to factor 2. This suggests that some fragments from the products of TBEP oxidation are likely similar to the products of CA oxidation or that a small fraction factor 4 is included in factor 2. Regardless, we conclude that factor 2 mainly represents the products of CA, while factor 4 represents the oxidation products of TBEP, since they are correspondingly anti-correlated with CA and TBEP in individual oxidation experiments. These results indicate that factors representing CA and TBEP can be effectively separated from their corresponding products.

The average mass spectra for these four factors are shown in Fig. 2. Strong intensities for mass channels at m/z 87 and 129 are present in factor 1 (CA), while strong signals at m/z 85, 125, 199, 227 and 299 are observed in factor 3 (TBEP). These fragments are in good agreement with the mass spectra of pure CA and TBEP respectively,

when compared with their NIST mass spectra (Fig. S2 in the Supplement). Figure 3a–d further compares the normalized mass spectra of factors 1 and 3 to pure CA and TBEP (atomized directly into the C-ToF-AMS). As shown in Fig. 3, the assignments of factors 1 and 3 above are well supported by the good correlation between the PMF mass spectra and the directly measured pure compound mass spectra across the entire mass range.

Furthermore, Fig. 2 demonstrates that the characteristic fragments of CA (m/z 87 and 129) are observable in factor 2, although at lower intensity than factor 1. The same is true for the characteristic fragments of TBEP (m/z 85, 125, 199, 227 and 299) in factor 4 when compared with factor 3 (Fig. 2). These results strongly suggest that factor 2 is mainly from the oxidation products of citric acid, and factor 4 from the oxidation products of TBEP, resulting in an overall 4 factor PMF solution.

3.2 PMF analysis for externally mixed CA and TBEP-AN (Exp. II)

The mass spectra of the non-oxidized, oxidized and the difference mass spectra (oxidized-non-oxidized) of externally mixed CA particles and TBEP-AN particles is shown in Fig. S3a–c in the Supplement. Consumption of both TBEP and CA is observed in Fig. S3c in the Supplement (shown as negative values in the difference spectrum). In order to perform kinetics calculations, the signals of TBEP and CA must be resolved from each other and from the various oxidation products. As described in Sect. 3.1, a two reactant and two product (ie: 4 factor) PMF solution is expected for this system, based upon separate experiments with CA and TBEP.

The temporal profiles of the 4-factor solution for the oxidation of externally mixed CA and TBEP-AN particles (Exp. II) are shown in Fig. 4. PMF analysis was performed combining the mass spectra obtained in Exp. I and II. In doing so, the assignment of factors for externally mixed particles in Exp. II is facilitated by directly comparing with those of Exp. I (reference spectra which are shaded on the left hand). As shown in Fig. 4, the 4-factor solution successfully separates the signals of CA, TBEP, and their

oxidation products, regardless of whether the particles were introduced into the reactor together (Exp. II) or via alternating particle sources (Exp. I).

It should be pointed out that the mathematical deconvolution of a dataset often yields non-unique solutions for PMF analysis, in which linear transformations (rotations) of the factors are possible while the positivity constraint is maintained (Ulbrich et al., 2009). Here we report the averaged fractional signals with different FPeaks (rotations) resulting in error bars which indicate the uncertainty of the PMF solution (Paatero, 2007). When exposed to OH radicals, the concentrations of CA (factor 1) and TBEP (factor 3) decrease synchronously with OH exposure, which was accompanied with an increase of factors 2 and 4. Similar trends were observed when internally mixed particles were oxidized as well; however the absolute kinetics were significantly different, as further discussed in the following section.

3.3 Derivation of kinetics

The vapor pressure of TBEP at 298 K is reported to range from 2.5×10^{-8} to 1.23×10^{-6} Torr (Veen and Boer, 2012; Verbruggen et al., 2005; Bergman et al., 2012; Brommer et al., 2014). The corresponding c^* ($c^* = PM/RT$, where P is the vapor pressure and M is the molecular weight of TBEP) ranges from 0.54 to 26.4 $\mu g\,m^{-3}$, which suggests that TBEP is semi-volatile. Consequently, based upon a simple partitioning model (Kroll and Seinfeld, 2008; Pankow, 1994), the particle-phase fraction of TBEP may vary from 27 % to 95 % when the mass loading of OA is 10 $\mu g\,m^{-3}$ (measured by the AMS in this study). This implies that the evaporation of TBEP from particles could potentially contribute to the decreases in particulate TBEP concentration observed as a function of OH exposure via the establishment of a new gas-particle equilibrium on the time scale of these experiments (52 s). Using a mass transfer diffusion model (Jacobson, 2005) combined with a partitioning model (Kroll and Seinfeld, 2008; Pankow, 1994) (described in detail in the Supplement), evaporation of TBEP is calculated to contribute less than 0.3 % to the particle-phase loss of TBEP within the residence time of our reactor (Fig. S5 in the Supplement). This is consistent with our previous conclusion

that evaporation of a different OPE, triphenyl phosphate (TPhP), is negligible in the reactor based on experiments even though it has a higher vapor pressure than TBEP (Liu et al., 2014b). This suggests that evaporation of TBEP in the reactor has little influence on kinetics calculations.

The relationship between the measured signals of TBEP and CA for externally mixed CA and TBEP-AN particles is shown in Fig. 5. The $\log c_{TBEP}/c_{TBEP,0}$ is linearly ($R > 0.96$) related to the $\log c_{CA}/c_{CA,0}$ according to Eq. (4) from which the apparent k_r of TBEP to CA is calculated to be 1.34 ± 0.04. The uncertainty is the standard deviation (σ) of repeat experiments. If specific tracer fragments (rather than PMF reactant factors) are used to represent the particle-phase concentration of CA (m/z 129) and TBEP (m/z 299), then k_r is underestimated by more than a factor of two (0.66 ± 0.13). The discrepancy between the two approaches has been discussed previously (Liu et al., 2014a). In order to obtain the true second-order rate constant ($k_{t,2}$), a gas-phase diffusion correction is necessary for mixed-phase reactions because concentration gradients of OH exist between gas-phase and particle-phase under ambient pressure, while it does not for the reaction between a gas-phase reference and OH radicals. A gas-phase diffusion correction for OH from gas-phase to the CA particle surface has been performed by applying a previously utilized empirical formula (Fuchs and Sutugin, 1970; Worsnop et al., 2002; Widmann and Davis, 1997). Additional gas-phase diffusion corrections for TBEP are unnecessary, as the k_r is approximately unity and the particle size for CA is the same as that of TBEP-AN in this study.

Kessler et al. have reported the k_2 for CA with respect to OH radical to be $(4.3 \pm 0.8) \times 10^{-13}$ cm^3 molecule s^{-1} at 308 K and 30 % RH (Kessler et al., 2012). Based upon a PMF analysis, however, we have measured the diffusion-corrected k_2 for CA to be $(3.31 \pm 0.29) \times 10^{-12}$ cm^3 molecule s^{-1} under the reaction conditions of the current study (298 K, (30 ± 3) % RH and similar OH levels) (Liu et al., 2014a). Using this value, the diffusion-corrected $k_{2,TBEP}$ is $(4.44 \pm 0.45) \times 10^{-12}$ cm^3 molecule s^{-1} according to

Eq. (4). The diffusion-corrected γ_{OH} is 1.57 ± 0.16 according to Eq. (5).

$$\gamma_{OH} = \frac{2D_p \rho_{TBEP} N_A}{3 v_{OH} M_{TBEP} k_{2,TBEP}} \quad (5)$$

Where D_p is the surface-weighted average particle diameter of unreacted particles (cm), ρ_{TBEP} is the density of TBEP (g cm^{-3}), N_A is Avogadro's number, v_{OH} is the average speed of OH radicals in the gas phase (cm s^{-1}), and M_{TBEP} is the molecular weight of the OPEs (g mol^{-1}). This value is comparable with the γ_{OH} on other types of organic aerosols (George et al., 2007; Hearn and Smith, 2006; Kessler et al., 2010; Lambe et al., 2007; Smith et al., 2009).

3.4 Influence of mixing state on TBEP oxidation (Exp. III)

in the ambient atmosphere, particles are often internally or externally mixed with other components (Jimenez et al., 2009), and it is well recognized that the mixing state or morphology of particles plays an important role in heterogeneous reaction kinetics (Rudich et al., 2007; Kuwata and Martin, 2012; Shiraiwa et al., 2011; Katrib et al., 2005; Zhou et al., 2012; Chan and Chan, 2013). The relative rates of TBEP to CA for internally mixed TBEP-CA particles and TBEP-CA-AN particles, respectively, are shown in Fig. 6a and b. In Fig. 6, the k_r of TBEP to CA for internally mixed particles increases greatly when compared with the externally mixed CA and TBEP-AN (Fig. 5). For internally mixed TBEP-CA particles (Fig. 6a), the k_r is 4.59 ± 0.12, and increases further to 19.53 ± 1.02 for internally mixed TBEP-CA-AN (Fig. 6b). The consumption of TBEP and CA relative to their corresponding initial concentrations from high to low OH exposure is shown in Fig. 7 in externally mixed CA and TBEP-AN (Fig. 7a), internally mixed TBEP-CA and TBEP-CA-AN (Fig. 7b and c) at 298 K and (30 ± 3) % RH. Oxidation of CA is significantly depressed in the internally mixed experiments (B and C), while TBEP oxidation is slightly enhanced.

Our previous work has demonstrated that OH exposures are reproducible within 15 % (Fig. S4 in the Supplement) when utilizing the same experimental conditions (RH, O_3 concentration and the flow rate) suggesting that the changes in k_r described above and in Figs. 5 and 6 are a result of the variations in the particle mixing state or morphology. For mixed-phase reactions, diffusion of the gas-phase oxidant through the particle surface has an important influence on reaction kinetics. For example, Katrib et al. (Katrib et al., 2005) found that the uptake coefficient (γ) of O_3 decreased significantly with increases in the lauric acid content, in a mixture of oleic and lauric acids due to a decrease in the diffusion coefficient of O_3. Zhou et al. (2012) also observed a decrease of γ_{O_3} when PAHs were coated with other organics. In the current study, TBEP is a surfactant, with a surface tension of 0.0342 N m^{-1} (Karsa, 1999), while CA has no significant effect on the surface tension (Theron and Lues, 2010). This suggests that TBEP may be enriched on the surface of internally mixed particles containing CA because the particles are generated by atomization followed by diffusion drying from liquid droplets. Consequently, TBEP is likely more accessible than CA to OH radicals for these internally mixed particles (Fig. 6, Exp. III). When compared with the internally mixed TBEP-CA (Fig. 6a), NH_4NO_3 (in internally mixed TBEP-CA-AN particles, Fig. 6b) further inhibits the oxidation of CA in TBEP-AN-CA which is consistent with CA being soluble in the aqueous phase NH_4NO_3 particles, whereas TBEP remains on the particle surface due to its surfactant properties. Thus, in the dry particles CA may be partially buried by NH_4NO_3 resulting in a core-shell morphology of the particle with respect to these two components. The presence of an AN coating may provide a barrier to the diffusion of OH in the particle phase, which is similar to that of O_3 in lauric acid-oleic acid particles (Katrib et al., 2005).

The changes in hygroscopicity and phase of the particle as a result of increased RH may also have an effect on the kinetics. Increased RH has been demonstrated to lead to decreases in the viscosity of the particle phase (Shiraiwa et al., 2011). This may promote the diffusion of OH or CA in the particle phase and lead to a faster apparent reaction. The relative rate of TBEP to CA in internally mixed TBEP-CA-AN particles at

an elevated RH (57 ± 2) % is given in Fig. 7c. The k_r in this case was 12.15 ± 1.82. This value is almost half that at (30 ± 3) % RH (ie: faster kinetics). Several recent studies have found that RH may significantly influence the phase of particles, and subsequently the mixing state and reactivity (Chan and Chan, 2013; Kuwata and Martin, 2012). This implies that the diffusion rate of CA or OH radicals in the particle phase increases at higher RH, subsequently enhancing the potential for reaction with OH. However, the k_r for internally mixed TBEP-CA-AN at (57 ± 2) % RH remains larger than that for externally mixed TBEP-AN and CA particles, suggesting that the internally mixed TBEP-CA-AN particles are partially softened by adsorbed water.

3.5 Atmospheric fate of TBEP

Although factors such as mixing state and RH described above affect the heterogeneous loss rates for TBEP, at the present time, the particle-phase kinetics for TBEP under any conditions are unavailable for comparison with the current results. Using the structure-activity-relationship (SAR) method combined with the Atmospheric Oxidation Program for Microsoft Windows (AOPWIN) model (US-EPA, 2000), which is widely used for risk assessment of priority chemicals, the gas phase k_2 with respect to OH for TBEP is estimated to be 1.29×10^{-10} cm^3 molecule s^{-1}. Watts and Linden (Watts and Linden, 2009) measured its k_2 toward OH in aqueous solution to be $(1.19 \pm 0.08) \times 10^{10}$ L mol^{-1} s^{-1}, which is equivalent to $(1.98 \pm 0.01) \times 10^{-11}$ cm^3 molecule s^{-1}. Hence, the heterogeneous rate constant for TBEP derived here is much lower than that in the gas or aqueous phases. In our previous work (Liu et al., 2014a), we have measured the heterogeneous k_2 of triphenyl phosphate (TPhP), tris-2-ethylhexyl phosphate (TEHP), and tris-1,3-dichloro-2-propyl phosphate (TDCPP) toward OH to be $(1.95 \pm 0.43) \times 10^{-12}$, $(4.25 \pm 0.78) \times 10^{-12}$ and $(1.35 \pm 0.35) \times 10^{-12}$ cm^3 molecule s^{-1}, respectively. The k_2 of TBEP is larger than those of TPhP and TDCPP, although they are of the same order of magnitude, and very close to that of TEHP. Using the AOPWIN model, the gas phase k_2 of TEHP is estimated to be 9.79×10^{-11} cm^3 molecule s^{-1},

which is also similar to that of TBEP (1.29×10^{-1} cm^3 molecule s^{-1}) and consistent with the fact that both TBEP and TEHP contain alkyl side chain groups which is likely the dominant reactive pathway. In ambient particles, the concentration of TBEP is often lower than other OPEs found in the remote regions (Möller et al., 2012), while it is comparable with that of other OPEs in urban areas (Salamova et al., 2013). The larger heterogeneous rate constant for TBEP in the current study may reasonably explain these observations. Assuming a 24 h average OH concentration of 1.0×10^6 molecules cm^{-3}, the particle-phase lifetime of TBEP is estimated to be approximately 2.2–2.9 days. This suggests that TBEP may undergo medium-range transport in the absence of other confounding factors.

However, in assessing the overall atmospheric fate and lifetime of TBEP (or any other particle phase compound), the partitioning to and from particles as a result ongoing gas-phase reactivity must be taken into account. While the influence of TBEP evaporation in the reactor is negligible, the residence time in the ambient atmosphere is many orders of magnitude longer (up to a week), and hence the evaporation process cannot be neglected for atmospheric lifetime estimations of semi-volatile organic compounds. Under such circumstances, the loss rate of TBEP will be affected by gas-phase degradation, evaporation (desorption) and uptake, as well as particle-phase degradation (measured in this study) if the evaporation has an intermediate rate compared with gas and particle phase degradation. We therefore investigate the overall lifetime of TBEP via the explicit modeling of these processes. The overall lifetimes of TPhP, TEHP and TDCPP are also discussed based upon our previously reported kinetics (Liu et al., 2014a).

The particle-phase and gas-phase loss rates of TBEP can be described by the following equations,

$$-\frac{dc_p}{dt} = k_{2,P}c_p c_{OH} + k_e c_p - k_a c_g(1-\theta) \quad (6)$$

$$-\frac{dc_g}{dt} = k_{2,g}c_g c_{OH} - k_e c_p + k_a c_g(1-\theta) \quad (7)$$

$$K_p = \frac{k_a}{k_e} = \frac{c_p}{c_g M} = \frac{1}{C^*} \quad (8)$$

Where $k_{2,p}$ and $k_{2,g}$ are the particle-phase and gas-phase second-order rate constant (cm^3 molecule s^{-1}), respectively; k_e and k_a are the evaporation rate and adsorption rate constants (s^{-1}), respectively; c_g and c_p are the gas-phase and particle-phase concentration of TBEP (molecules cm^{-3}); c_{OH} is the concentration of OH in the atmosphere (molecules cm^{-3}); M is the mass concentration of organic matter in the particle-phase (μg m^{-3}); K_p is the partition coefficient of TBEP (m^3 μg^{-1}) and C^* is the saturated vapor pressure of TBEP (μg m^{-3}); θ is the surface coverage of TBEP.

Given that the concentration of TBEP in particles is on the order of several ng m^{-3} (Carlsson et al., 1997), it is reasonable to assume $\theta \ll 1$. Thus,

$$\frac{d\ln c_p}{dt} = k_{2,P}c_{OH} + k_e - \frac{k_e}{M} \quad (9)$$

The value of k_e was calculated with a mass transfer model for drops (Jacobson, 2005) and a gas-particle partition model (Kroll and Seinfeld, 2008; Pankow, 1994). The details with respect to the model and inputs are described in Table S1 in the Supplement. Finally, an estimated overall atmospheric lifetime (τ) can be calculated as,

$$\tau = \frac{1}{k_{2,P}c_{OH} + k_e - \frac{k_e}{M}} \quad (10)$$

Figure 8a illustrates the influence of evaporation rate on the overall atmospheric lifetime of TBEP assuming an average OH concentration of 1×10^6 molecules cm^{-3}. The blue line is the particle-phase loss curve using the measured k_2 of 4.44×10^{-12} cm^3 $molecule^{-1}$ s^{-1} without considering evaporation and gas-phase loss. The red line represents the gas-phase degradation of TBEP. The corresponding lifetimes of TBEP (gas or particle-phase) are 2.6 and 0.09 days (2.2 h). The k_e for TBEP is also estimated in the model (Supplement) for $PM_{1.0}$ (1 µm), $PM_{0.5}$ (500 nm) and $PM_{0.2}$ (200 nm), assuming 5 µg m^{-3} of organic matter (Vogel et al., 2013) and 1 ng m^{-3} of TBEP in urban particle matter which is on the same order of indoor dust (2.2–5.9 ng m^{-3}) (Carlsson et al., 1997) as inputs. The corresponding k_e values are 3.80×10^{-7}, 8.10×10^{-7} and 2.18×10^{-6} s^{-1}, from which the atmospheric lifetime of TBEP is estimated to be 2.4, 2.3 and 1.9 days, respectively, and are somewhat shorter than the value obtained directly from the experiments of this study (2.6 days). The corresponding results for TEHP and TDCPP are also shown in Fig. 8b and c based on their $k_{2,p}$ reported previously (Liu et al., 2014a). The lifetime of TEHP varies from 2.4 to 2.7 days, while it is 1.9–8.1 days for TDCPP when evaporation has been considered. In the case of TPhP, the apparent first-order degradation rate calculated according to Eq. (9) for 200 nm particles is larger than the gas-phase degradation rate (1.10×10^{-5} s^{-1}) due to the high vapor pressure (the lower limit of 4.77×10^{-5} Pa, Brommer et al., 2014). Even for 1000 nm particles, the overall lifetime of TPhP is estimated as 2.0 days. This suggests that gas phase degradation of TPhP should be the dominant loss process in the atmosphere, while the estimated lifetimes for other OPEs studied here are dominated by particle phase degradation.

It should be noted that the overall lifetime estimated here depends upon the value of k_e and k_{2p}. k_e is sensitive to particle size and vapor pressure of OPEs. A wide range of vapor pressures for these OPEs have been summarized in a recent work (Brommer et al., 2014). In our work, we have used the lower limit of vapor pressure as inputs in the evaporation model. Apart from the uncertainty of the vapor pressure measurements, the evaporation model will likely overestimate the evaporation kinetics of OA

(Vaden et al., 2011). An ideal solution is assumed in the current model, while interaction between OPEs and other matrices in the ambient atmosphere will likely decrease the k_e value for OPEs, leading to a longer lifetime. Furthermore, recent studies have found that SOA is a semisolid phase with high viscosity (Abramson et al., 2013; Vaden et al., 2011) and that aged SOA demonstrated a slower evaporation rate than fresh or uncoated SOA (Vaden et al., 2011). If OPEs are internally mixed with or coated by SOA (resulting in a core-shell morphology) during transport, the evaporation rate of OPEs may be further reduced, and/or the reactivity of OPEs towards OH may be slowed (as observed in reactions of benzo[a]pyrene and O_3 coated with SOA (Zhou et al., 2013) and TPhP coated with oxalic acid (Liu et al., 2014b). In particular, the measurements of TPhP in PM in remote regions (Möller et al., 2012), despite its dominant gas-phase loss contribution (based upon our model results) highlights the effect of multi-component particle mixtures on the kinetics of particle degradation. Thus, the results presented here are likely a lower bound of the true atmospheric lifetimes.

4 Implications and conclusions

Using a particle-phase relative rates technique, the second-order rate constant of TBEP toward OH is measured to be $(4.44 \pm 0.45) \times 10^{-12}$ cm^3 $molecule^{-1}$ s^{-1} at 298 K and (30 ± 3) % RH resulting in a particle-phase lifetime of TBEP estimated to be 2.2–2.9 days. Explicitly modeling the overall atmospheric lifetime of OPEs suggests that evaporation of OPEs from particles will reduce their atmospheric lifetime further. However, the derived heterogeneous rate constants and the explicit model results are in contrast to observations that show many OPEs can undergo long range transport. This is consistent with the large differences in the relative rate constants for TBEP when comparing internally and externally mixed particles and upon changes in the RH. These results have important implications for the modeling of OPE fate in the atmosphere. Foremost, they demonstrate that the heterogeneous degradation of TBEP (or other compounds in PM) may be depressed or enhanced depending upon the surfactant nature of the

species relative to the matrix in which it is immersed, the RH conditions experienced by the particle, and the amount and/or nature of further atmospheric organic coatings. Secondly, the lifetime of OPEs (as demonstrated in the model results) will also significantly depend upon particle size when the partitioning process of TBEP is considered during transport. Finally, a proper risk assessment of this and other SVOC compounds must include the gas-particle partitioning process, and ideally eventually include the effect of other components of the particle on the evaporation kinetics and/or the heterogeneous loss rates.

The Supplement related to this article is available online at doi:10.5194/acpd-14-19431-2014-supplement.

Acknowledgements. This research was financially supported by the Chemicals Management Plan (CMP) and the Clean Air Regulatory Agenda (CARA).

References

Abbatt, J. P. D., Lee, A. K. Y., and Thornton, J. A.: Quantifying trace gas uptake to tropospheric aerosol: recent advances and remaining challenges, Chem. Soc. Rev., 41, 6555–6581, doi:10.1039/c2cs35052a, 2012.

Abramson, E., Imre, D., Beranek, J., Wilson, J., and Zelenyuk, A.: Experimental determination of chemical diffusion within secondary organic aerosol particles, Phys. Chem. Chem. Phys., 15, 2983–2991, doi:10.1039/c2cp44013j, 2013.

Ali, N., Dirtu, A. C., Eede, N. V. D., Goosey, E., Harrad, S., Neels, H., Mannetje, A. T., Coakley, J., Douwes, J., Covaci, A.: Occurrence of alternative flame retardants in indoor dust from New Zealand: indoor sources and human exposure assessment, Chemosphere, 88, 1276–1282, 2012.

Badger, C. L., Griffiths, P. T., George, I., Abbatt, J. P. D., and Cox, R. A.: Reactive uptake of N_2O_5 by aerosol particles containing mixtures of humic acid and ammonium sulfate, J. Phys. Chem. A, 110, 6986–6994, 2006.

Barnes, I. and Rudzinski, K. J.: Environmental Simulation Chambers: Application to Atmospheric Chemical Processes, Springer, P.O. Box 17, 3300 AA Dordrecht, the Netherlands, 2006.

Bergman, Å., Rydén, A., Law, R. J., de Boer, J., Covaci, A., Alaee, M., Birnbaum, L., Petreas, M., Rose, M., Sakai, S., Van den Eede, N., and van der Veen, I.: A novel abbreviation standard for organobromine, organochlorine and organophosphorus flame retardants and some characteristics of the chemicals, Environ. Int., 49, 57–82, 2012.

Brommer, S., Jantunen, L. M., Bidleman, T. F., Harrad, S., and Diamond, M. L.: Determination of vapor pressures for organophosphate esters, J. Chem. Eng. Data, 59, 1441–1447, doi:10.1021/je401026a, 2014.

Cappa, C. D., Che, D. L., Kessler, S. H., Kroll, J. H., and Wilson, K. R.: Variations in organic aerosol optical and hygroscopic properties upon heterogeneous OH oxidation, J. Geophys. Res., 116, D15204, doi:10.1029/2011jd015918, 2011.

Carlsson, H., Nilsson, U., Becker, G., and Östman, C.: Organophosphate ester flame retardants and plasticizers in the indoor environment: analytical methodology and occurrence, Environ. Sci. Technol., 31, 2931–2936, doi:10.1021/es970123s, 1997.

Cequier, E., Ionas, A. C., Covaci, A., Marcé, R. M., Becher, G., and Thomsen, C.: Occurrence of a broad range of legacy and emerging flame retardants in indoor environments in Norway, Environ. Sci. Technol., 48, 6827–6835, doi:10.1021/es500516u, 2014.

Chan, L. P. and Chan, C. K.: Role of the aerosol phase state in ammonia/amines exchange reactions, Environ. Sci. Technol., 47, 5755–5762, 2013.

Crowley, J. N., Ammann, M., Cox, R. A., Hynes, R. G., Jenkin, M. E., Mellouki, A., Rossi, M. J., Troe, J., and Wallington, T. J.: Evaluated kinetic and photochemical data for atmospheric chemistry: Volume V – heterogeneous reactions on solid substrates, Atmos. Chem. Phys., 10, 9059–9223, doi:10.5194/acp-10-9059-2010, 2010.

Dishaw, L. V., Powers, C. M., Ryde, I. T., Roberts, S. C., Seidler, F. J., Slotkin, T. A., and Stapleton, H. M.: Is the PentaBDE replacement, tris (1,3-dichloro-2-propyl) phosphate (TDCPP), a developmental neurotoxicant? Studies in PC12 cells, Toxicol. Appl. Pharm., 256, 281–289, 2011.

Dodson, R. E., Perovich, L. J., Covaci, A., Eede, N. V. D., Ionas, A. C., Dirtu, A. C., Brody, J. G., and Rudel, R. A.: After the PBDE phase-Out: a broad suite of flame retardants in repeat house dust samples from California, Environ. Sci. Technol., 46, 13056–13066, 2012.

Donahue, N. M., Robinson, A. L., Hartz, K. E. H., Sage, A. M., and Weitkamp, E. A.: Competitive oxidation in atmospheric aerosols: the case for relative kinetics, Geophys. Res. Lett., 32, L16805, doi:10.1029/2005gl022893, 2005.

EPA, US: Furniture Flame Retardancy Partnership: Environmental Profiles of Chemical Flame-Retardant Alternatives for Low-Density Polyurethane Foam, Environmental Protection Agency, Sep, available at: www.epa.gov/dfe (last access: 23 September 2012), 2005.

Frinak, E. K., Wermeille, S. J., Mashburn, C. D., Tolbert, M. A., and Pursell, C. J.: Heterogeneous reaction of gaseous nitric acid on γ-Phase Iron(III) oxide, J. Phys. Chem. A, 108, 1560–1566, doi:10.1021/jp030807o, 2004.

Fuchs, N. A. and Sutugin, A. G.: Highly Dispersed Aerosols, Butterworth-Heinemann, Newton, MA, 1970.

George, I. J. and Abbatt, J. P. D.: Heterogeneous oxidation of atmospheric aerosol particles by gas-phase radicals, Nat. Chem., 2, 713–722, doi:10.1038/nchem.806, 2010a.

George, I. J. and Abbatt, J. P. D.: Chemical evolution of secondary organic aerosol from OH-initiated heterogeneous oxidation, Atmos. Chem. Phys., 10, 5551–5563, doi:10.5194/acp-10-5551-2010, 2010b.

George, I. J., Vlasenko, A., Slowik, J. G., Broekhuizen, K., and Abbatt, J. P. D.: Heterogeneous oxidation of saturated organic aerosols by hydroxyl radicals: uptake kinetics, condensed-phase products, and particle size change, Atmos. Chem. Phys., 7, 4187–4201, doi:10.5194/acp-7-4187-2007, 2007.

Han, C., Liu, Y., and He, H.: Role of organic carbon in heterogeneous reaction of NO_2 with soot, Environ. Sci. Technol., 47, 3174–3181, doi:10.1021/es304468n, 2013.

Hanisch, F. and Crowley, J. N.: Ozone decomposition on Saharan dust: an experimental investigation, Atmos. Chem. Phys., 3, 119–130, doi:10.5194/acp-3-119-2003, 2003.

Heald, C. L., Kroll, J. H., Jimenez, J. L., Docherty, K. S., DeCarlo, P. F., Aiken, A. C., Chen, Q., Martin, S. T., Farmer, D. K., and Artaxo, P.: A simplified description of the evolution of organic aerosol composition in the atmosphere, Geophys. Res. Lett., 37, L08803, doi:10.1029/2010GL042737, 2010.

Hearn, J. D. and Smith, G. D.: A mixed-phase relative rates technique for measuring aerosol reaction kinetics, Geophys. Res. Lett., 33, L17805, doi:10.1029/2006gl026963, 2006.

IPCS (International Programme on Chemical Safety): Flame Retardants: Tri(2-Butoxyethyl) Phosphate, Tris(2-Ethylhexyl) Phosphate and Tetrakis(Hydroxymethyl) Phosphonium Salts, Environmental Health Criteria, 218, World Health Organization, Geneva, Switzerland, 2000.

Jacobson, M. Z.: Fundamentals of Atmospheric Modeling, Cambridge University Press, Cambridge, UK, 2005.

Jimenez, J. L., Canagaratna, M. R., Donahue, N. M., Prevot, A. S. H., Zhang, Q., Kroll, J. H., DeCarlo, P. F., Allan, J. D., Coe, H., Ng, N. L., Aiken, A. C., Docherty, K. S., Ulbrich, I. M., Grieshop, A. P., Robinson, A. L., Duplissy, J., Smith, J. D., Wilson, K. R., Lanz, V. A., Hueglin, C., Sun, Y. L., Tian, J., Laaksonen, A., Raatikainen, T., Rautiainen, J., Vaattovaara, P., Ehn, M., Kulmala, M., Tomlinson, J. M., Collins, D. R., Cubison, M. J., Dunlea, E. J., Huffman, J. A., Onasch, T. B., Alfarra, M. R., Williams, P. I., Bower, K., Kondo, Y., Schneider, J., Drewnick, F., Borrmann, S., Weimer, S., Demerjian, K., Salcedo, D., Cottrell, L., Griffin, R., Takami, A., Miyoshi, T., Hatakeyama, S., Shimono, A., Sun, J. Y., Zhang, Y. M., Dzepina, K., Kimmel, J. R., Sueper, D., Jayne, J. T., Herndon, S. C., Trimborn, A. M., Williams, L. R., Wood, E. C., Middlebrook, A. M., Kolb, C. E., Baltensperger, U., and Worsnop, D. R.: Evolution of organic aerosols in the atmosphere, Science, 326, 1525–1529, 2009.

Kanakidou, M., Seinfeld, J. H., Pandis, S. N., Barnes, I., Dentener, F. J., Facchini, M. C., Van Dingenen, R., Ervens, B., Nenes, A., Nielsen, C. J., Swietlicki, E., Putaud, J. P., Balkanski, Y., Fuzzi, S., Horth, J., Moortgat, G. K., Winterhalter, R., Myhre, C. E. L., Tsigaridis, K., Vignati, E., Stephanou, E. G., and Wilson, J.: Organic aerosol and global climate modelling: a review, Atmos. Chem. Phys., 5, 1053–1123, doi:10.5194/acp-5-1053-2005, 2005.

Karsa., D. R.: Design and Selection of Performance Surfactants, Sheffield Academic Press, P260, Sheffield, UK, 1999.

Katrib, Y., Biskos, G., Buseck, P. R., Davidovits, P., and Jayne, J. T.: Ozonolysis of mixed oleic-acid/stearic-acid particles: reaction kinetics and chemical morphology, J. Phys. Chem. A, 109, 10910–10919, 2005.

Kessler, S. H., Smith, J. D., Che, D. L., Worsnop, D. R., Wilson, K. R., and Kroll, J. H.: Chemical sinks of organic aerosol: kinetics and products of the heterogeneous oxidation of erythritol and levoglucosan, Environ. Sci. Technol., 44, 7005–7010, doi:10.1021/es101465m, 2010.

Kessler, S. H., Nah, T., Daumit, K. E., Smith, J. D., Leone, S. R., Kolb, C. E., Worsnop, D. R., Wilson, K. R., and Kroll, J. H.: OH-initiated heterogeneous aging of highly oxidized organic aerosol, J. Phys. Chem. A, 116, 6358–6365, doi:10.1021/jp212131m, 2012.

Kolb, C. E. and Worsnop, D. R.: Chemistry and composition of atmospheric aerosol particles, Annu. Rev. Phys. Chem., 63, 471–491, doi:10.1146/annurev-physchem-032511-143706, 2012.

Kolb, C. E., Cox, R. A., Abbatt, J. P. D., Ammann, M., Davis, E. J., Donaldson, D. J., Garrett, B. C., George, C., Griffiths, P. T., Hanson, D. R., Kulmala, M., McFiggans, G., Pöschl, U., Riipinen, I., Rossi, M. J., Rudich, Y., Wagner, P. E., Winkler, P. M., Worsnop, D. R., and O' Dowd, C. D.: An overview of current issues in the uptake of atmospheric trace gases by aerosols and clouds, Atmos. Chem. Phys., 10, 10561–10605, doi:10.5194/acp-10-10561-2010, 2010.

Kroll, J. H. and Seinfeld, J. H.: Chemistry of secondary organic aerosol: formation and evolution of low-volatility organics in the atmosphere, Atmos. Environ., 42, 3593–3624, 2008.

Kuwata, M. and Martin, S. T.: Phase of atmospheric secondary organic material affects its reactivity, P. Natl. Acad. Sci. USA, 109, 17354–17359, 2012.

Lambe, A. T., Zhang, J. Y., Sage, A. M., and Donahue, N. M.: Controlled OH radical production via ozone-alkene reactions for use in aerosol aging studies, Environ. Sci. Technol., 41, 2357–2363, doi:10.1021/es061878e, 2007.

Liggio, J., Li, S.-M., Vlasenko, A., Stroud, C., and Makar, P.: Depression of ammonia uptake to sulfuric acid aerosols by competing uptake of ambient organic gases, Environ. Sci. Technol., 45, 2790–2796, doi:10.1021/es103801g, 2011.

Liu, C., Zhang, P., Wang, Y., Yang, B., and Shu, J.: Heterogeneous reactions of particulate methoxyphenols with NO_3 radicals: kinetics, products, and mechanisms, Environ. Sci. Technol., 46, 13262–13269, 2012.

Liu, Y., Ma, Q., and He, H.: Heterogeneous uptake of amines by citric acid and humid acid, Environ. Sci. Technol., 46, 11112–11118, doi:10.1021/es302414v, 2012.

Liu, Y., Li, S.-M., and Liggio, J.: Application of positive matrix factor analysis in heterogeneous kinetics studies: an improvement to the mixed-phase relative rates technique, Atmos. Chem. Phys. Discuss., 14, 8695–8722, doi:10.5194/acpd-14-8695-2014, 2014a.

Liu, Y., Liggio, J., Harner, T., Jantunen, L., Shoeib, M., and Li, S.-M.: Heterogeneous OH initiated oxidation: a possible explanation for the persistence of organophosphate flame retardants in air, Environ. Sci. Technol., 48, 1041–1048, 2014b.

Möller, A., Xie, Z., Caba, A., Sturm, R., and Ebinghaus, R.: Organophosphorus flame retardants and plasticizers in the atmosphere of the North Sea, Environ. Pollut., 159, 3660–3665, 2011.

Möller, A., Sturm, R., Xie, Z., Cai, M., He, J., and Ebinghaus, R.: Organophosphorus flame retardants and plasticizers in airborne particles over the Northern Pacific and Indian Ocean toward the polar regions: evidence for global occurrence, Environ. Sci. Technol., 46, 3127–3134, 2012.

McNeill, V. F., Wolfe, G. M., and Thornton, J. A.: The Oxidation of oleate in submicron aqueous salt aerosols: evidence of a surface process, J. Phys. Chem. A, 111, 1073–1083, 2007.

McNeill, V. F., Yatavelli, R. L. N., Thornton, J. A., Stipe, C. B., and Landgrebe, O.: Heterogeneous OH oxidation of palmitic acid in single component and internally mixed aerosol particles: vaporization and the role of particle phase, Atmos. Chem. Phys., 8, 5465–5476, doi:10.5194/acp-8-5465-2008, 2008.

Mogili, P. K., Kleiber, P. D., Young, M. A., and Grassian, V. H.: N_2O_5 hydrolysis on the components of mineral dust and sea salt aerosol: comparison study in an environmental aerosol reaction chamber, Atmos. Environ., 40, 7401–7408, 2006.

Ndour, M., D'Anna, B., George, C., Ka, O., Balkanski, Y., Kleffmann, J., Stemmler, K., and Ammann, M.: Photoenhanced uptake of NO_2 on mineral dust: laboratory experiments and model simulations, Geophys. Res. Lett., 35, L05812, doi:10.1029/2007gl032006, 2008.

Paatero, P.: Least squares formulation of robust non-negative factor analysis, Chemom. Intell. Lab. Syst., 37, 23–35, doi:10.1016/S0169-7439(96)00044-5, 1997.

Paatero, P.: User's Guide for Positive Matrix Factorization Programs PMF2.EXE and PMF3.EXE, University of Helsinki, Helsinki, Finland, 2007.

Paatero, P. and Tapper, U.: Positive matrix factorization: a nonnegative factor model with optimal utilization of error estimates of data values, Environmetrics, 5, 111–126, 1994.

Pankow, J. F.: An absorption-model of gas-particle partitioning of organic compounds in the atmosphere, Atmos. Environ., 28, 185–188, 1994.

Pöschl, U.: Atmospheric aerosols: composition, transformation, climate and health effects, Angew. Chem. Int. Edit., 44, 7520–7540, doi:10.1002/anie.200501122, 2005.

Qiu, C., Wang, L., Lal, V., Khalizov, A. F., and Zhang, R.: Heterogeneous reactions of alkylamines with ammonium sulfate and ammonium bisulfate, Environ. Sci. Technol., 45, 4748–4755, 2011.

Ravishankara, A. R.: Heterogeneous and multiphase chemistry in the troposphere, Science, 276, 1058–1065, 1997.

Reemtsma, T., García-López, M., Rodríguez, I., Quintana, J. B., and Rodil, R.: Organophosphorus flame retardants and plasticizers in water and air, I. Occurrence and fate, Trends Analyt. Chem., 27, 727–737, 2008.

Regnery, J. and Püttmann, W.: Organophosphorus flame retardants and plasticizers in rain and snow from middle Germany, Clean-Soil Air Water, 37, 334–342, 2009.

Renbaum, L. H. and Smith, G. D.: Artifacts in measuring aerosol uptake kinetics: the roles of time, concentration and adsorption, Atmos. Chem. Phys., 11, 6881–6893, doi:10.5194/acp-11-6881-2011, 2011.
Romanias, M. N., Zein, A. E., and Bedjanian, Y.: Reactive uptake of HONO on aluminium oxide surface, J. Photoch. Photobio. A, 250, 50–57, 2012.
Rudich, Y., Donahue, N. M., and Mentel, T. F.: Aging of organic aerosol: bridging the gap between laboratory and field studies, Annu. Rev. Phys. Chem., 58, 321–352, doi:10.1146/annurev.physchem.58.032806.104432, 2007.
Salamova, A., Ma, Y., Venier, M., and Hites, R. A.: High levels of organophosphate flame retardants in the great lakes atmosphere, Environ. Sci. Technol. Lett., 1, 8–14, doi:10.1021/ez400034n, 2013.
Salamova, A., Hermanson, M. H., and Hites, R. A.: Organophosphate and halogenated flame retardants in atmospheric particles from a European Arctic site, Environ. Sci. Technol., 48, 6133–3140, doi:10.1021/es500911d, 2014.
Sareen, N., Moussa, S. G., and McNeill, V. F.: Photochemical aging of light-absorbing secondary organic aerosol material, J. Phys. Chem. A, 117, 2987–2996, 2013.
Shiraiwa, M., Ammann, M., Koop, T., and Pöschl, U.: Gas uptake and chemical aging of semisolid organic aerosol particles, P. Natl. Acad. Sci. USA, 108, 11003–11008, doi:10.1073/pnas.1103045108, 2011.
Smith, J. D., Kroll, J. H., Cappa, C. D., Che, D. L., Liu, C. L., Ahmed, M., Leone, S. R., Worsnop, D. R., and Wilson, K. R.: The heterogeneous reaction of hydroxyl radicals with sub-micron squalane particles: a model system for understanding the oxidative aging of ambient aerosols, Atmos. Chem. Phys., 9, 3209–3222, doi:10.5194/acp-9-3209-2009, 2009.
Tang, M. J., Thieser, J., Schuster, G., and Crowley, J. N.: Uptake of NO_3 and N_2O_5 to Saharan dust, ambient urban aerosol and soot: a relative rate study, Atmos. Chem. Phys., 10, 2965–2974, doi:10.5194/acp-10-2965-2010, 2010.
Theron, M. M. and Lues, J. F. R.: Organic Acids and Food Preservation, CRC Press, P128, Boca Raton, USA, 2010.
Ulbrich, I. M., Canagaratna, M. R., Zhang, Q., Worsnop, D. R., and Jimenez, J. L.: Interpretation of organic components from Positive Matrix Factorization of aerosol mass spectrometric data, Atmos. Chem. Phys., 9, 2891–2918, doi:10.5194/acp-9-2891-2009, 2009.

Ullerstam, M., Johnson, M. S., Vogt, R., and Ljungström, E.: DRIFTS and Knudsen cell study of the heterogeneous reactivity of SO_2 and NO_2 on mineral dust, Atmos. Chem. Phys., 3, 2043–2051, doi:10.5194/acp-3-2043-2003, 2003.
US-EPA: Atmospheric Oxidation Program for Microsoft Windows (AOPWIN), Environmental Protection Agency, Washington D.C., USA, 2000.
Vaden, T. D., Imre, D., Beránek, J., Shrivastava, M., and Zelenyuk, A.: Evaporation kinetics and phase of laboratory and ambient secondary organic aerosol, P. Natl. Acad. Sci. USA, 108, 2190–2195, doi:10.1073/pnas.1013391108, 2011.
v. d. Veen, I. and d. Boer, J.: Phosphorus flame retardants: properties, production, environmental occurrence, toxicity and analysis, Chemosphere, 88, 1119–1153, 2012.
Verbruggen, E. M. J., Rila, J. P., Traas, T. P., Posthuma-Doodeman, C. J. A. M., and Posthumus, R.: Environmental Risk Limits for Several Phosphate Esters, with Possible Application as Flame Retardant, RIVM report 601501024, Bilthoven, the Netherlands, 2005.
Vogel, A. L., Äijälä, M., Corrigan, A. L., Junninen, H., Ehn, M., Petäjä, T., Worsnop, D. R., Kulmala, M., Russell, L. M., Williams, J., and Hoffmann, T.: In situ submicron organic aerosol characterization at a boreal forest research station during HUMPPA-COPEC 2010 using soft and hard ionization mass spectrometry, Atmos. Chem. Phys., 13, 10933–10950, doi:10.5194/acp-13-10933-2013, 2013.
Watts, M. J. and Linden, K. G.: Advanced oxidation kinetics of aqueous trialkyl phosphate flame retardants and plasticizers, Environ. Sci. Technol., 43, 2937–2942, 2009.
WHO: Environmental Health Criteria 218, Flame Retardants: Tris(2-Butoxyethyl) Phosphate, Tris(2-Ethylexyl) Phosphate And Tetrakis(Hydroxymethyl) Phosphonium Salts, World Health Organization, Geneva, 2000.
Widmann, J. F. and Davis, E. J.: Mathematical models of the uptake of $ClONO_2$ and other gases by atmospheric aerosols, J. Aerosol Sci., 28, 87–106, 1997.
Worsnop, D. R., Morris, J. W., Shi, Q., Davidovits, P., and Kolb, C. E.: A chemical kinetic model for reactive transformations of aerosol particles, Geophys. Res. Lett., 29, 1996, doi:10.1029/2002gl015542, 2002.
Zhang, Q., Jimenez, J., Canagaratna, M., Ulbrich, I., Ng, N., Worsnop, D., and Sun, Y.: Understanding atmospheric organic aerosols via factor analysis of aerosol mass spectrometry: a review, Anal. Bioanal. Chem., 401, 3045–3067, doi:10.1007/s00216-011-5355-y, 2011.
Zhang, Y. and Carmichael, G.: Interactions of mineral aerosol with tropospheric chemistry, J. Appl. Meteorol., 38, 353–366, 1999.

Zhou, S., Lee, A. K. Y., McWhinney, R. D., and Abbatt, J. P. D.: Burial effects of organic coatings on the heterogeneous reactivity of particle-borne benzo[a]pyrene (BaP) toward ozone, J. Phys. Chem. A, 116, 7050–7056, doi:10.1021/jp3030705, 2012.

Zhou, S., Shiraiwa, M., McWhinney, R. D., Poschl, U., and Abbatt, J. P. D.: Kinetic limitations in gas-particle reactions arising from slow diffusion in secondary organic aerosol, Faraday Discuss., 165, 391–406, doi:10.1039/c3fd00030c, 2013.

Table 1. Experimental details for oxidation experiments.

Exp.	Mixing state	Components	D_m (nm)	Objectives
I	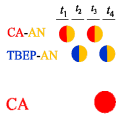	CA-AN or TBEP-AN	210	Reference spectra for PMF analysis; resolving ability of PMF
II		CA and TBEP-AN	210	Kinetics of TBEP
III		TBEP-CA or TBEP-CA-AN	210	Influence of mixing state on kinetics

Note: CA-AN: internally mixed citric acid and ammonium nitrate; TBEP-AN: internally mixed TBEP and AN; TBEP-CA-AN: internally mixed TBEP, CA and AN.

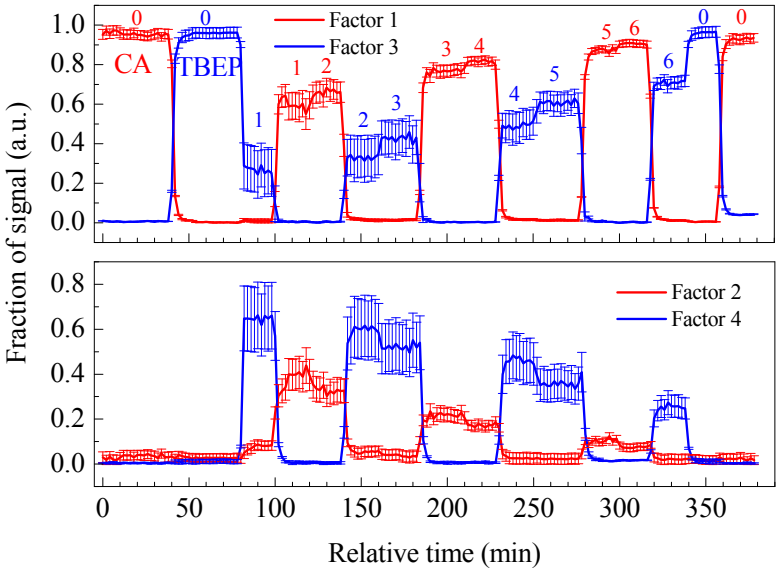

Figure 1. Averaged concentration profiles of the 4-factor solution for individually oxidized TBEP-AN and CA-AN particles. The number "0" represents an OH exposure of zero, while the numbers from "1" to "6" represent OH exposure decreases from $7.8 \pm 0.8 \times 10^{11}$ to $8.5 \pm 0.8 \times 10^{10}$ molecules cm^{-3} s. Exp 1, 2, 3 represent three repeat experiments.

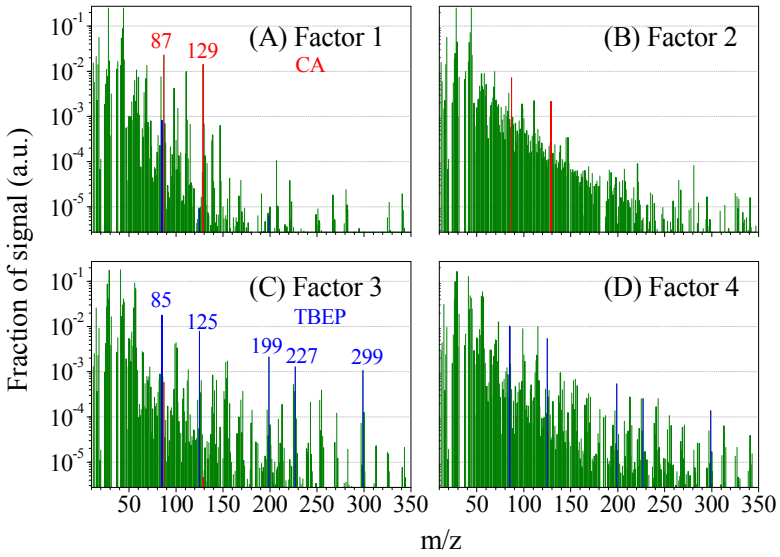

Figure 2. Averaged mass spectra of the 4-factor solution for individually oxidized TBEP-AN and CA-AN particles. The red lines indicate the characteristic fragments of CA, while the blue lines are those for TBEP.

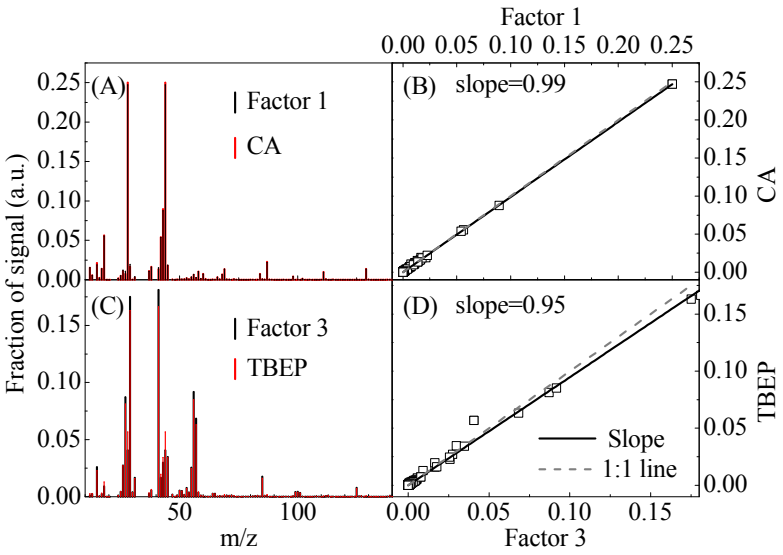

Figure 3. Comparison of the mass spectra extracted by PMF analysis and those measured through direct atomization.

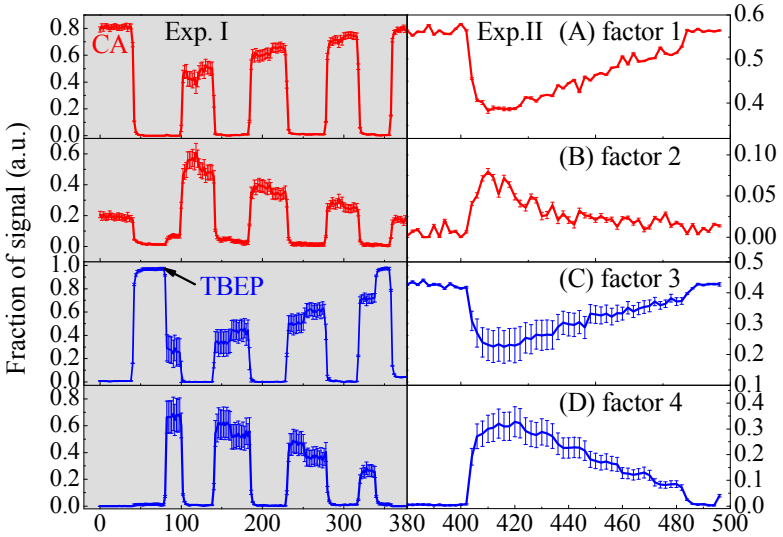

Figure 4. Typical temporal concentration profiles of the 4-factor solution for oxidation of externally mixed TBEP-AN and CA particles. On the left shaded column, the curves are the same as those in Fig. 1 (Exp. I); they are for oxidizing externally mixed TBEP -NH_4NO_3 and CA on the right column (Exp. II).

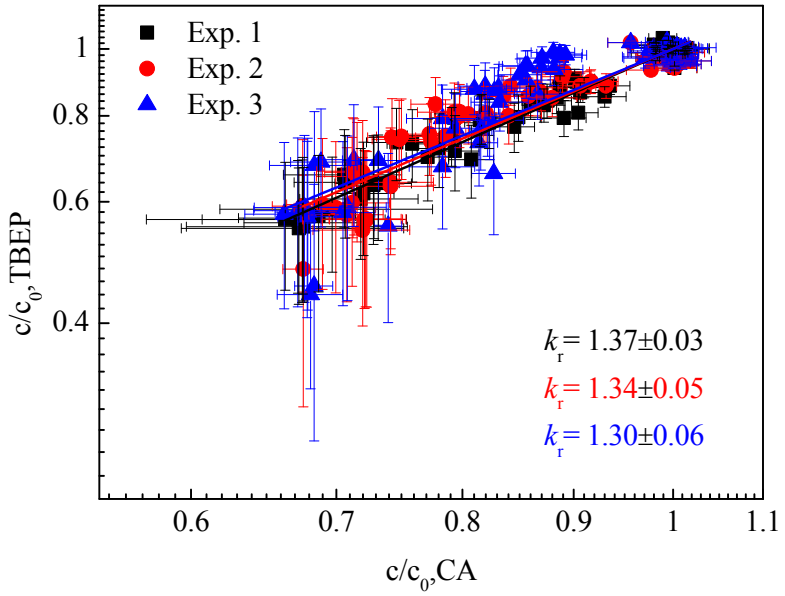

Figure 5. Relative rates for externally mixed CA and TBEP-AN at 298 K and (30 ± 3) % RH.

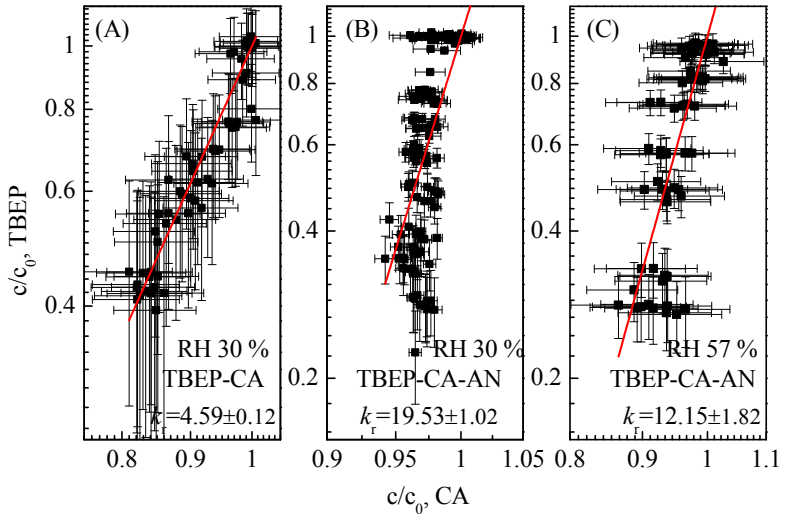

Figure 6. Comparison of the relative rates for internally mixed **(A)** TBEP-CA and **(B)** TBEP-CA-AN at 298 K and (30 ± 3) % RH, and **(C)** TBEP-CA-AN at 298 K and (57 ± 2) % RH.

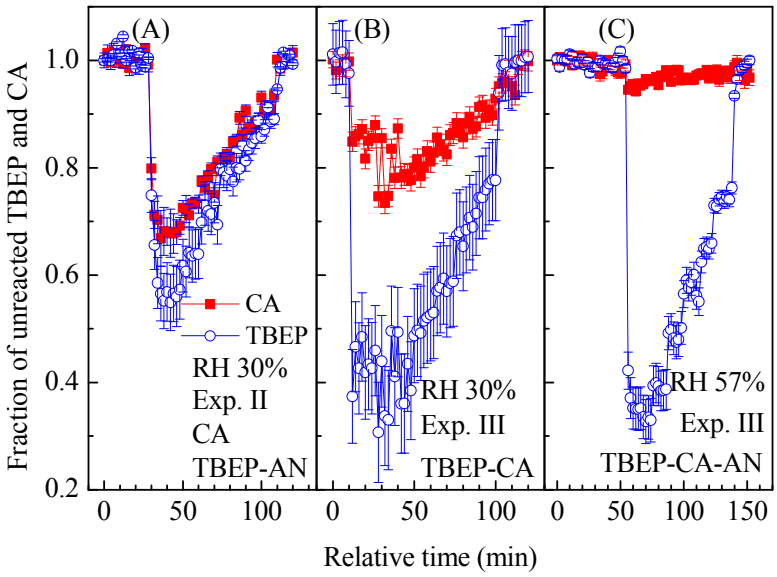

Figure 7. Comparison for the c/c_0 of TBEP and CA in **(A)** externally mixed CA and TBEP-AN, **(B)** internally mixed TBEP-CA, and **(C)** internally mixed TBEP-CA-AN at 298 K and (30 ± 3) % RH.

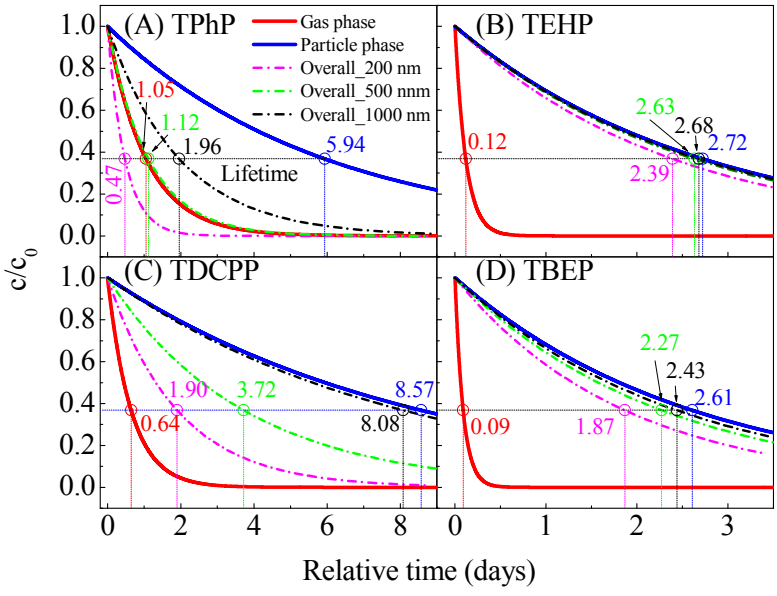

Figure 8. Influence of evaporation from particles of various diameter on the particle-phase loss rate of **(A)** TPhP, **(B)** TEHP, **(C)** TDCPP and **(D)** TBEP.